Devil's staircase and harmless staircase in the smectic-C_α^* phase in an electric field

Barbara Rovšek,[1,2] Mojca Čepič,[1,3] and Boštjan Žekš[1,4]
[1]*Jožef Stefan Institute, Jamova 39, 1000 Ljubljana, Slovenia*
[2]*Faculty of Mathematics and Physics, Jadranska 19, 1000 Ljubljana, Slovenia*
[3]*Faculty of Education, Kardeljeva ploščad 16, 1000 Ljubljana, Slovenia*
[4]*Institute of Biophysics, Medical Faculty, Lipičeva 2, 1000 Ljubljana, Slovenia*
(Received 13 February 2004; published 28 October 2004)

The unwinding of the short pitch helical smectic-C_α^* structure in an external electric field is studied within a discrete phenomenological model. It is found that the pitch increases quasicontinuously at low electric fields and is commensurate with the smectic layer thickness at any field. The sequence of stable structures recalls the once popular and then abandoned devil's staircase model. At larger fields the pitch grows discontinuously in steps of one smectic layer, forming a harmless staircase. Taking into account the achiral next-nearest-layer interactions the final transition to the unwound structure is found to be discontinuous.

DOI: 10.1103/PhysRevE.70.041706 PACS number(s): 61.30.Cz

Elongated chiral molecules of polar smectics form layered structures. If molecules are tilted with respect to the smectic plane, it can be concluded by symmetry arguments that the smectic layers are polar. This theoretical argument almost 30 years ago led to the synthesis of the first ferroelectric liquid crystals [1]. Fifteen years ago, in the search for materials with higher polarization, antiferroelectric liquid crystals were discovered [2]. Their phase diagram revealed several different phases which remain experimental and theoretical challenges today.

In this paper we concentrate on the smectic-C_α^* (Sm-C_α^*) phase. For many years it was explained as a set of structures where molecules in adjacent layers form a periodic pattern of synclinic and anticlinic tilt boundaries. The period was suggested to range from a few up to ten and more layers. By changing the temperature or applied electric field the repetitive pattern and its length were reported to change discontinuously [3]. The phase diagram obtained was interpreted as a devil's staircase [3–7]. Later, the devil's staircase model was disproved when the results of resonant x-ray scattering experiments, a method that enabled direct structural observations in layered smectics [8], were found to be consistent with the predictions of a discrete phenomenological model of the Sm-C_α^* phase [9,10]. It was experimentally confirmed that the Sm-C_α^* phase has a tilted, short pitch helicoidally modulated structure with the pitch in general incommensurate with the smectic layer thickness. The model is now called the clock model of the Sm-C_α^* phase.

In this article we show that the first tentative explanations of the Sm-C_α^* phase should not be considered as completely inconsistent. When an incommensurate short pitch Sm-C_α^* phase is exposed to an external electric field, its structure deforms and locks to commensurate periods. The unwinding process at small electric fields consists of stepwise structural changes between commensurate structures, typical for the devil's staircase behavior. At larger fields, when approaching the critical field for complete unwinding, discontinuous changes reveal the harmless staircase behavior [7]. The results are consistent with the experiments [3] that motivated the introduction of the first devil's staircase models for the Sm-C_α^* phase. We compare the continuous and discrete formalisms and discuss the appropriateness of their application in different circumstances.

The helicoidally modulated layered structure of the Sm-C_α^* phase in an external electric field is described by the tilt order parameter $\boldsymbol{\xi}_i$. In the free energy, only the terms that account for interlayer interactions and the coupling with the electric field are present,

$$G_{il}=\sum_i\left(\frac{1}{2}a_1\boldsymbol{\xi}_i\cdot\boldsymbol{\xi}_{i+1}+\frac{1}{2}f\boldsymbol{\xi}_i\times\boldsymbol{\xi}_{i+1}+\frac{1}{8}a_2\boldsymbol{\xi}_i\cdot\boldsymbol{\xi}_{i+2}-\mathbf{E}\cdot\mathbf{P}_i\right). \tag{1}$$

The a_1 and f terms account for the achiral and chiral interactions between the nearest-neighboring layers [9]. The achiral next-nearest-layer interactions are described by the a_2 term. The signs of the parameters a_1 and a_2 determine the preferred relative orientation of tilts in interacting layers. If a_1 and a_2 are positive, anticlinic tilts are favored, and if they are negative, synclinic tilts are favored. The chiral interactions always induce a helical variation of tilt along the layer normal. The last term in Eq. (1) describes the coupling of piezoelectric polarization $\mathbf{P}_i=(\boldsymbol{\xi}_i\times\mathbf{n}_i)P_0$ of each smectic layer with the external field. The polarization $\mathbf{P}_i$ is perpendicular to the average tilt of the molecules in a particular layer and proportional to the magnitude of the tilt, and $\mathbf{n}_i$ is the layer normal.

The equilibrium structure is given by a set of tilts $\boldsymbol{\xi}_i=\theta_i\{\cos\phi_i,\sin\phi_i\}$, where θ_i is a magnitude and ϕ_i describes the direction of the tilt in the ith smectic layer. For $\mathbf{E}=\mathbf{0}$, the stable structure is helicoidally modulated: the phase difference of tilts in neighboring layers is a constant $\alpha=\phi_{i+1}-\phi_i$ and $\theta_i=\theta_0$ for any i. When we insert the expected form of the stable solution into the expression (1), the free energy becomes

$$G_{il}(\alpha)=\frac{\theta_0^2}{2}\sum_i\left(a_1\cos\alpha+f\sin\alpha+\frac{a_2}{4}\cos 2\alpha\right). \tag{2}$$

The phase difference α_0 that minimizes Eq. (2) for a chosen set of model parameters solves the equation

 ©2004 The American Physical Society

$$f = a_1 \tan \alpha_0 + a_2 \sin \alpha_0. \tag{3}$$

The stable structure is helicoidal, with the zero-field pitch $p_0 = 2\pi d/\alpha_0 = N_0 d$, where d is the smectic layer thickness and N_0 is some real number. In general p_0 is incommensurate with d. Expressing f and a_2 in units of $|a_1|$, we are left with two parameters $f/|a_1|$ and $a_2/|a_1|$ which define the zero-field pitch. We stress that for any given p_0 infinite combinations of model parameters $a_2/|a_1|$ and $f/|a_1|$ can be found satisfying Eq. (3).

An external electric field that is parallel to the smectic layer influences the structure. We do not consider the minor influence on the magnitude of the tilt, i.e., the electroclinic effect. Minimizing the bulk free energy (1) with respect to the set of tilt phase angles ϕ_i gives a set of nonlinear equations. Although the pitch extends over a few layers only, it is in general incommensurate with the layer thickness and the number of equations is therefore infinite.

In the numerical procedure inevitably only a finite number of equations can be treated. The finite number of equations and appropriate boundary conditions do not allow the period of the structure to change. However, we expect the pitch to grow with the field. We solved the problem of the growing period by taking several ideal helices as the initial approximations of the zero-field structure. The helical structures have different pitches $p_{P,Q}$ all commensurate with the smectic layer thickness and therefore representable with rational numbers, $p_{P,Q} = (P/Q)d$. The integer P is the commensurate period and Q is the winding number of the structure. Periodic boundary conditions reduce the number of equations to a controllable number. We analyze how various zero-field helical structures transform in the electric field by iteratively solving a linearized set of equations. At $\mathbf{E} \neq \mathbf{0}$ the given zero-field structure is deformed within one pitch, but the pitch remains the same.

We check a variety of pitches (up to $P = 200$ and $Q = 5$) and calculate and compare the energies of the corresponding structures. The structure with the least energy among the structures we have studied is close enough to the equilibrium structure. Important general conclusions can be drawn on the basis of our results.

The numerical minimization shows that all the calculated structures have domains formed by adjacent layers which have a component of polarization in the direction of the electric field (Fig. 1). The domains are separated from each other by domain walls, which are formed by a few layers that have an unfavorable orientation of polarization with a component opposite to **E**. We found that all domain walls are similar, almost symmetric around the most unfavorable orientation of polarization antiparallel to **E**. There are always two neighboring layers in the middle of each domain wall, which have polarizations approximately at angles $\pi \pm \beta$ with respect to the direction of **E** (see Fig. 1).

We call the region from the middle of a domain wall to the middle of the next domain wall a subperiod. At any field, any calculated structure with pitch $p_{P,Q}$ is built only from subperiods with $M_{P,Q}$ and $M_{P,Q}+1$ layers, where $M_{P,Q}$ is the integer part of P/Q. Not even in a single layer of any structure is the polarization perfectly antiparallel to **E**. This is the origin of the appearance of the commensurate period of the stable structure also, which locks to the integer number of smectic layers. It is energetically favorable to build subperiods which differ in lengths by one layer and have similar domain walls, and this is a general conclusion.

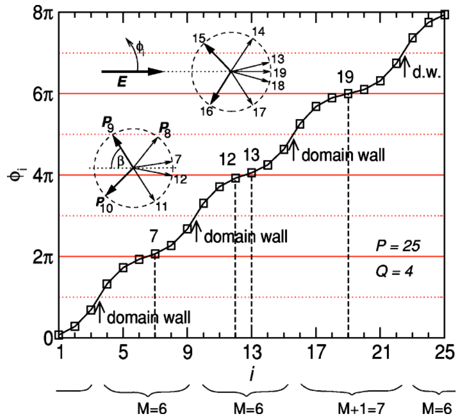

FIG. 1. Deformed helical structure in the presence of electric field, for $p_0 = 5$ layers, $a_1 = -1$ K, $a_2/|a_1| = 0.3$, $f/|a_1| = -2.79$, and $E = 1.19$ kV/mm. Commensurate period P extends over 25 layers and consists of three subperiods of six and one of seven layers, $Q = 4$. The structures of two domain walls are shown on the insets. One is between two subperiods with six layers (ninth and tenth layers), and the other between subperiods with six and seven layers (15th and 16th layers).

At a certain field (the closest to) the equilibrium structure is the one with the minimum energy among all that were calculated. The commensurate period P of the stable structure consists of j subperiods of length M and k subperiods of length $M+1$. The integers j and k do not have a common divisor, and if one of them is 0, the other one is 1, and $j + k = Q$. There are $jM + k(M+1)$ layers in one period P. The pitch p of the structure is the average length of the subperiod within one period P. With growing electric field, j and k change so the portion of longer subperiods $k/(j+k)$ increases until eventually all subperiods have the same length of $M+1$ layers. On further increasing the field, subperiods with $M+2$ layers appear. The sequence of stable structures in an increasing electric field is the devil's staircase. The process is essentially discontinuous but the commensurate period P can be long, with a large number of subperiods within it. The experimental observations would inevitably show a continuous dependence on observable quantities. Therefore we call this process *quasicontinuous*.

At large fields close to the critical field E_d, where the structure eventually unwinds completely, all subperiods have the same length. The pitch p of the minimum energy structure locks to the integer number of smectic layers and further on increases in steps of one layer. We call the process *stepwise* unwinding and it is similar to harmless step behavior [7]. The final step can be either drastically discontinuous, from some finite length pitch below E_d to infinite in the unwound structure above E_d if a_2 is large, or stepwise, if a_2 is small or zero (see Fig. 2).

From Fig. 2 we also see that different combinations of $a_2/|a_1|$ and $f/|a_1|$ which all define the same zero-field pitch

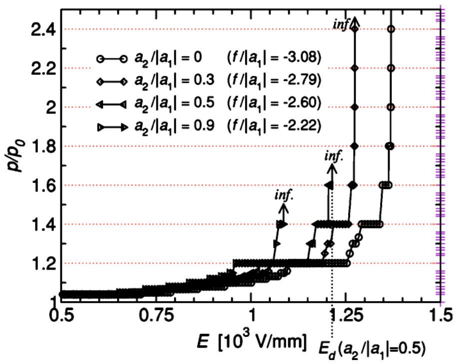

FIG. 2. The pitch grows with the field as is shown here for a structure with $p_0=5$ layers. For the material and model parameters appropriate values were taken, representing a typical substance forming the Sm-C_α^* phase: $P_0=100\ \mathrm{nC/cm^2}, \theta_0=\pi/20$, and $a_1/a=-1$ K where $a=4\times10^4\ \mathrm{J/m^3}$ [13]. The parameter a_2 was varied between 0 and $|a_1|$, and f was defined by Eq. (3) to lead to $p_0=5$ layers in every case. At low fields the pitch grows quasicontinuously and jumps discontinuously in steps of one layer at large fields. At critical field E_d the structure unwinds completely. The pitch grows faster with $\mathbf{E}$ if a_2 is larger. The curves end at critical field E_d. Discrete jumps of the pitch at low fields are numerical artifacts, due to finite discreteness of the pitch net. The commensurate pitches, which were checked, are marked at the right side of the plot.

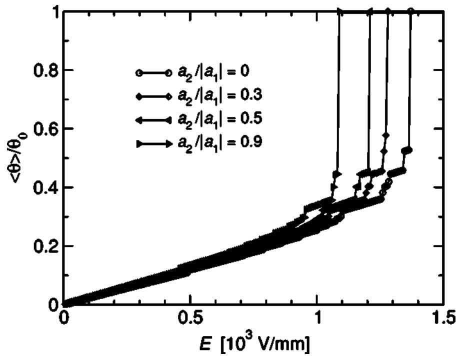

FIG. 3. Induced apparent tilt angle $\langle\theta\rangle$ in dependence on the electric field, for the structure with $p_0=5$ layers and different values of the parameter a_2.

and therefore the same zero-field structure lead to much different evolution of the pitch with the field. Two general conclusions are made. The first: the larger the contribution of the achiral next-nearest-layer interactions a_2, the faster the pitch grows with the field. And the second: the final transition to the unwound planar structure at critical field E_d also becomes discontinuous, and the larger the a_2 the lower the critical field.

The reason for the described behavior is the symmetry of the bulk free energy (2) in dependence on the phase difference α. With only the nearest-neighbor interactions (when $a_2=0$) the free energy $G_{il}(\alpha)$ is symmetric around the minimum, which defines the equilibrium α_0. The energy costs for additional uniform twisting or unwinding of the helix for the same $\Delta\alpha$ are the same. A balance between the elastic forces stabilizing the helical structure and the electrostatic forces stabilizing the unwound structure is achieved in the absence of next-nearest-layer interactions in a continuous distortion and unwinding of the helical structure in the electric field until it is unwound completely (Fig. 2, the curve, corresponding to $a_2=0$). If $a_2\neq0$, the symmetry around the minimum is lost. In general, unwinding becomes energetically favorable; therefore the unwound regions grow faster with the field, and the domain walls also become wider. The consequence is a discontinuous transition to completely unwound structure at some critical field E_d, where the index d stands for the analysis on the basis of a discrete model [9].

Discontinuous changes of pitch result in stepwise changes of the apparent tilt angle $\langle\theta\rangle$ which are presented in Fig. 3. Additional consideration of the electroclinic effect would smooth the calculated dependence of $\langle\theta\rangle$, but mostly at high fields close to the critical field for complete unwinding. The apparent tilt dependence on the electric field obtained would then nicely reproduce the experimentally observed dependence in [3]: The reported stepwise increase of $\langle\theta\rangle$ can be clearly seen from the plot of $\partial\langle\theta\rangle/\partial E$ in dependence on E therein and therefore lends support to our model. To our knowledge there are no other experiments providing such direct evidence for discontinuous changes of the pitch with electric field.

We also examined the limitations of the continuum model [11,12], which was widely applied in studies of the long pitch helical structure of the Sm-C^* phase. A link between the discrete and continuum models can be obtained by continuization of the discrete model around the equilibrium bulk helical structure. The relevant phase-angle-dependent part of the continuum expansion of the bulk free energy density is usually written as [11]

$$g_\phi(z)=\frac{1}{2}K\theta^2\left(\frac{d\phi}{dz}\right)^2-\Lambda\theta^2\frac{d\phi}{dz}-EP\cos\phi,$$

where K is the elastic constant, Λ is the Lifshitz parameter, and P is the magnitude of polarization, proportional to the tilt θ, $P=\theta P_0$. Using discrete forms of derivatives, the discrete model is translated to a continuum model and we get the relations between the parameters

$$K=-\frac{d}{2}\left(\frac{a_1}{\cos\alpha_0}+a_2\cos^2\alpha_0\right)\quad\text{and }\Lambda=Kq_0,$$

where $q_0=\alpha_0/d$ describes the zero-field equilibrium helical structure. The specific influences of each of the three parameters of the discrete model (a_1,a_2, and f) are hidden, when combined into two parameters of the continuum model (K and Λ). The critical field E_c, where the complete continuous unwinding of the helix occurs in the continuum model [12], written with the parameters of a discrete model is

$$E_c=\left(\frac{\pi}{4}\right)^2\frac{K\theta^2q_0^2}{P}=-\left(\frac{\pi}{4}\right)^2\frac{\theta\alpha_0^2}{2dP_0}\left(\frac{a_1}{\cos\alpha_0}+a_2\cos^2\alpha_0\right).$$

The results of the discrete model were compared to the predictions of the continuum model. The critical field E_d found numerically in the discrete model is smaller than the corresponding critical field within the continuum model E_c. The

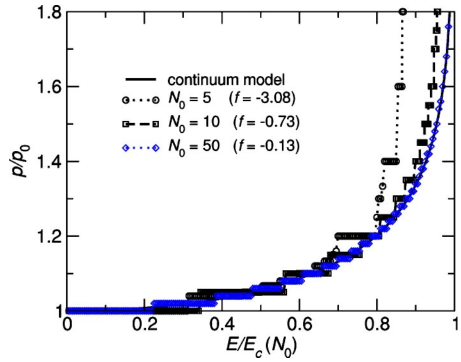

FIG. 4. Comparison of the results obtained from discrete and continuum calculations for helical structures with different pitches and a_2 equal to zero. The larger the pitch, the closer are the results of the two models.

larger a_2, the larger the difference between these two fields, and also, the shorter the pitch, the larger is the difference between E_c and E_d. This is an expected result: the continuum expansion is appropriate, if variations of the order parameter from layer to layer are small, which is not true for a short pitch structure (Fig. 4).

To conclude, we found that the unwinding process of the short pitch structure of the Sm-C_α^* phase in the external electric field reveals both a quasicontinuous devil's staircase sequence locked to the commensurate periodical structures at lower fields and a stepwise harmless staircase at fields close to the critical electric field for complete unwinding. The next-nearest interactions, described by the a_2 term in the discrete model of antiferroelectric liquid crystals, strongly influence the behavior of the helical short pitch smectic structure. Large next-nearest interactions in general decrease the critical electric field E_d, as well as the critical field in the continuum model E_c. The difference between the E_c and numerically obtained E_d is larger if next-nearest-layer interactions are larger. We see that two helical structures with the same zero-field pitch behave differently in an electric field, if next-nearest-layer interactions are different for them.

In the absence of an electric field the helical pitch is defined by different microscopic interactions: chiral nearest layers of van der Waals origin and effective achiral next-nearest layers of flexoelectric and electrostatic origin [9]. For a long time it was believed that chiral interlayer interactions, described by f, are weak in comparison with achiral next-nearest-layer interactions, described by a_2. Since both types of interaction have the same effect on the structure—they both favor the formation of the helix—it was impossible to experimentally separate their influence on the structure. The analysis presented paves the way for indirect observations of the f/a_2 ratio. The pitch of the zero-field structure can be obtained by detailed ellipsometric measurements [10,14] or resonant x-ray scattering [8] on thick (to minimize the influence of the surfaces) free standing films. For the same material the apparent tilt in dependence on the electric field can be measured [3] in planar cells and compared with the theoretical predictions for different ratios f/a_2.

The research was supported by the Ministry of Education, Science and Sport of Slovenia (Grant No. Z1-3292).

[1] R.B. Meyer, L. Liebert, L. Strzelecki, and P. Keller, J. Phys. (France) Lett. **36**, L69 (1975).
[2] A.D.L. Chandani, E. Gorecka, Y. Ouchi, H. Takezoe, and A. Fukuda, Jpn. J. Appl. Phys., Part 2 **28**, L1265 (1989).
[3] K. Hiraoka, Y. Takanishi, K. Skarp, H. Takezoe, and A. Fukuda, Jpn. J. Appl. Phys., Part 2 **30**, L1819 (1991); K. Hiraoka, Y. Takanishi, H. Takezoe, A. Fukuda, T. Isozaki, Y. Suzuki, and I. Kawamura, Jpn. J. Appl. Phys., Part 1 **31**, 3394 (1992).
[4] P. Bak, Phys. Today **39**(12), 38 (1986).
[5] Y. Takanishi, K. Hiraoka, V.K. Agrawal, H. Takezoe, A. Fukuda, and M. Matsushita, Jpn. J. Appl. Phys., Part 1 **30**, 2023 (1991); T. Isozaki, T. Fujikawa, H. Takezoe, A. Fukuda, T. Hagiwara, Y. Suzuki, and I. Kawamura, Phys. Rev. B **48**, 13 439 (1993); A. Roy and N. V. Madhusudana, Europhys. Lett. **41**, 501 (1998).
[6] M. Yamashita and S. Miyazima, Ferroelectrics **148**, 1 (1993); M. Yamashita, Mol. Cryst. Liq. Cryst. Sci. Technol., Sect. A **263**, 93 (1995); M. Yamashita, J. Phys. Soc. Jpn. **67**, 198 (1998).
[7] P.M. Chaikin and T.C. Lubensky, *Principles of Condensed Matter Physics* (Cambridge University Press, Cambridge, England, 1995).
[8] P. Mach, R. Pindak, A.-M. Levelut, P. Barois, H.T. Nguyen, C.C. Huang, and L. Furenlid, Phys. Rev. Lett. **81**, 1015 (1998).
[9] M. Čepič and B. Žekš, Mol. Cryst. Liq. Cryst. Sci. Technol., Sect. A **263**, 61 (1995); **301**, 221 (1997); Phys. Rev. Lett. **87**, 085501 (2001).
[10] B. Rovšek, M. Čepič, and B. Žekš, Phys. Rev. E **54**, R3113 (1996).
[11] S.A. Pikin and V.L. Indenbom, Ferroelectrics **20**, 151 (1978).
[12] B. Urbanc, B. Žekš, and T. Carlsson, Ferroelectrics **113**, 219 (1991).
[13] I. Muševič, R. Blinc, and B. Žekš, *The Physics of Ferroelectric and Antiferroelectric Liquid Crystals* (World Scientific, Singapore, 2000).
[14] Ch. Bahr and D. Fliegner, Phys. Rev. Lett. **70**, 1842 (1993); D.A. Olson, S. Pankratz, P.M. Johnson, A. Cady, H.T. Nguyen, and C.C. Huang, Phys. Rev. E **63**, 061711 (2001).